Proteolytic processing of Middle East respiratory syndrome coronavirus spikes expands virus tropism

Jung-Eun Park[a], Kun Li[b], Arlene Barlan[a], Anthony R. Fehr[c], Stanley Perlman[b,c], Paul B. McCray Jr.[b,c], and Tom Gallagher[a,1]

[a]Department of Microbiology and Immunology, Loyola University Chicago, Maywood, IL 60153; [b]Department of Pediatrics, University of Iowa, Iowa City, IA 52242; and [c]Department of Microbiology, University of Iowa, Iowa City, IA 52242

Edited by Peter Palese, Icahn School of Medicine at Mount Sinai, New York, NY, and approved September 13, 2016 (received for review May 20, 2016)

Middle East respiratory syndrome coronavirus (MERS-CoV) infects humans from zoonotic sources and causes severe pulmonary disease. Virions require spike (S) glycoproteins for binding to cell receptors and for catalyzing virus–cell membrane fusion. Fusion occurs only after S proteins are cleaved sequentially, first during their secretion through the exocytic organelles of virus-producing cells, and second after virus binding to target-cell receptors. To more precisely determine how sequential proteolysis contributes to CoV infection, we introduced S mutations obstructing the first cleavages. These mutations severely compromised MERS-CoV infection into human lung-derived cells, but had little effect on infection into several other cell types. These cell type-specific requirements for proteolysis correlated with S conformations during cell entry. Without the first cleavages, S proteins resisted cell receptor-induced conformational changes, which restricted the second, fusion-activating cleavages. Consistent with these findings, precleaved MERS viruses used receptor-proximal, cell-surface proteases to effect the second fusion-activating cleavages during cell entry, whereas the more rigid uncleaved MERS viruses trafficked past these cell-surface proteases and into endosomes. Uncleaved viruses were less infectious to human airway epithelial and Calu3 cell cultures because they lacked sufficient endosomal fusion-activating proteases. Thus, by sensitizing viruses to receptor-induced conformational changes, the first S cleavages expand virus tropism to cell types that are relevant to lung infection, and therefore may be significant determinants of MERS-CoV virulence.

coronavirus | virus entry | receptor | protease

Enveloped viruses deposit their genomes into host cells by coalescing their membranes with the cell. These functions are executed by virion envelope-anchored glycoprotein trimers termed "membrane-fusion proteins." In virus-infected cells, these proteins are synthesized as inactive forms, structured such that they can maintain their membrane-fusion potential throughout their residence on extracellular virus particles. The proteins then transit into fusion-competent forms during virus-cell entry. Various environmental stimuli control these cell entry-related structural transitions. Proteolysis is central, as fusion proteins cleaved by host proteases are frequently liberated to undergo transitions into fusion-competent forms (1–3). Knowledge of the proteolytic cleavages and host proteases regulating virus infections can be used to predict viral tropism and pathogenesis (4, 5), and can also reveal antiviral strategies (6).

Coronaviruses (CoVs) are enveloped, positive-stranded RNA viruses in the order *Nidovirales*. These viruses infect mammals and birds, and are mainly associated with respiratory and enteric tract disorders (7). Of six known human CoVs, the severe acute respiratory syndrome (SARS)-CoV and Middle East respiratory syndrome (MERS)-CoV are the most recent to have emerged from zoonotic reservoirs, which include bats (8–10), Himalayan palm civets and other animals found in wet markets in China (11, 12), and Dromedary camels (13). Infection can cause acute respiratory distress with high mortality, particularly in elderly individuals and those with underlying pulmonary dysfunctions (14, 15). It is unknown whether the spread of these highly pathogenic CoVs between animals and humans, as well as within the infected respiratory system, relates to their propensity to use particular lung proteases as entry factors.

CoV fusion proteins, called spike (S) proteins, are integral-membrane ∼500-kDa trimers that project ∼20 nm from viral envelopes (Fig. 1*A*). Atomic resolution structures of two CoV S protein ectodomains have recently been obtained (16, 17). These structures can be broadly divided into receptor-binding domains (RBDs in Fig. 1*A*), and fusion-catalyzing domains (FDs in Fig. 1*A*). For MERS-CoV, the S RBDs bind to dipeptidyl peptidase 4 (DPP4/CD26) receptors (18). Following receptor binding, the FDs are revealed through unfolding transitions, such that viral fusion peptides (FP in Fig. 1*B*) intercalate into host cell membranes. Subsequent refolding transitions bring viral and cellular membranes so close that they coalesce.

The unfolding of the FDs is thought to require S protein cleavage by host proteases (19). Although the MERS-CoV S proteins have several proteolytic cleavage sites between the RBDs and FDs, a scission at the S1/S2 site (Fig. 1*B*) takes place in virus-producing cells, by furin or related proprotein convertases (20). Subsequent proteolyses at more C-terminal sites, notably the S2′ site (Fig. 1*B*), takes place later in the virus transmission process, after virions have been released from producing cells and bound to target-cell receptors (1, 21, 22). These proteases include members of type II transmembrane serine proteases (TTSPs) (23, 24), furin/proprotein convertases (21, 25), and cathepsins (23, 26).

Proteolysis at S2′ is thought to trigger S-mediated membrane fusion. Therefore, the abundance and subcellular distribution of the TTSPs, furin/proprotein convertases, and cathepsins quite likely determines host cell susceptibility to CoV infection, as well as the tempo and site of CoV fusion into cells (19). In contrast, the relevance of the S1/S2 proteolysis to CoV infection is more ambiguous. For example, several infectious CoVs lack S1/S2

Significance

Middle East respiratory syndrome coronavirus (MERS-CoV) can cause lethal pneumonia by infecting lung epithelial cells. Infection requires viral "spike" proteins, which catalyze virus–cell membrane fusion during cell entry. Fusion catalysis requires that spikes be first cleaved by cellular proteases. MERS-CoV spikes are cleaved in virus-producing cells before subsequent virus-cell entry, whereas other human coronaviruses have spikes that are cleaved in virus-infecting cells during virus-cell entry. Here, we found that the early MERS-CoV cleavages are required for the subsequent infection of human lung-like cells, but are dispensable for infection of several other cell types. Our findings demonstrate that the spike cleavage status of MERS-CoVs dictates cell tropism, and points to spike proteolytic processing as a correlate of MERS-CoV virulence.

Author contributions: J.-E.P., K.L., A.R.F., and T.G. designed research; J.-E.P., K.L., A.B., and A.R.F. performed research; S.P. and P.B.M. contributed new reagents/analytic tools; J.-E.P., S.P., P.B.M., and T.G. analyzed data; and J.-E.P. and T.G. wrote the paper.

The authors declare no conflict of interest.

This article is a PNAS Direct Submission.

[1]To whom correspondence should be addressed. Email: tgallag@luc.edu.

This article contains supporting information online at www.pnas.org/lookup/suppl/doi:10.1073/pnas.1608147113/-/DCSupplemental.

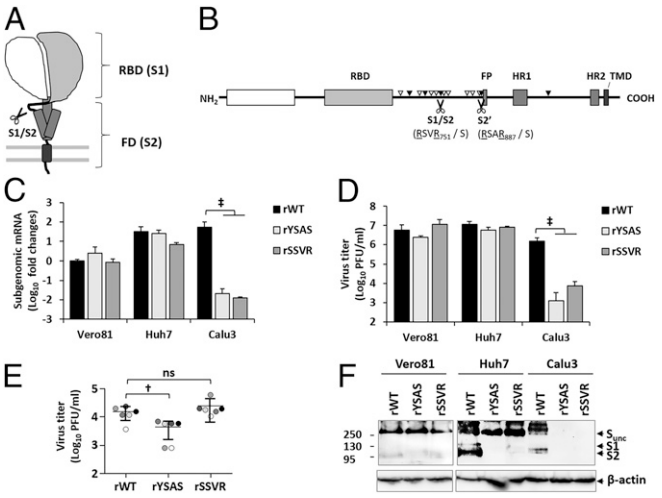

Fig. 1. S1/S2 cleavage is required for MERS-CoV infection of Calu3 cells. (*A*) CoV particles have ∼100 S trimers. A single CoV S monomer is highlighted. A globular RBD (S1) and a stem-like FD (S2) is separated by domains that include the S1/S2 cleavage site. (*B*) A linear depiction of the MERS-CoV S protein includes a RBD, FP, two heptad repeats (HR1 and HR2), and a transmembrane domain (TMD). Two known proteolytic cleavage sites (S1/S2 and S2′) are depicted. Additional putative furin/proprotein convertase (black arrow heads) and cathepsin (white arrow heads) cleavage sites were predicted by ProP 1.0 Server (www.cbs.dtu.dk/services/ProP/) and SitePrediction (www.dmbr.ugent.be/prx/bioit2-public/SitePrediction/index.php), respectively. (*C*) Vero81, Huh7, and Calu3 cells were infected with WT and S1/S2 mutant (YSAS and SSVR) MERS-CoVs. After 5 h, subgenomic N mRNAs were determined by real-time PCR, and plotted relative to N mRNA levels in WT MERS-CoV–infected Vero81 cells. (*D*) Vero81, Huh7, and Calu3 cells were infected with WT and S1/S2 mutant MERS-CoVs. Progeny were collected at 20-h postinfection and titrated by plaque assay in Vero81 cells. (*E*) Six HAE cultures were infected with WT and S1/S2 mutant MERS-CoVs. Progeny were collected at 20-h postinfection and titrated by plaque assay in Vero81 cells. Error bars present SD from the mean ($n = 3$ for cultured cells, $n = 6$ for HAE cultures). Statistical significance was assessed by Student's *t* test. $^{\dagger}P < 0.01$; $^{\ddagger}P < 0.001$; ns, not significant. (*F*) Vero81, Huh7, and Calu3 cells were infected with WT and S1/S2 mutant MERS-CoVs and S proteins within cells were analyzed by Western blot. Uncleaved (S_{unc}) and cleaved (S1 and S2) positions are indicated. The numbers at the left indicate molecular mass in kilodaltons.

proteolytic processing motifs and therefore secrete from producer cells as uncleaved forms (27, 28). For those CoVs with S1/S2 processing sites, mutation of the sites to block the cleavages often does not abrogate viral infectivity (20, 29). Pharmacologic inhibition of proprotein convertases diminished preliminary MERS-CoV S1/S2 cleavages, but did not reduce viral infectivity into several cell types (30).

We hypothesized that S1/S2 proteolysis in virus-producing cells facilitates subsequent S2′ cleavage by fusion-activating proteases in virus target cells. An extension of this hypothesis was that the S1/S2 proteolysis might determine which target-cell proteases (TTSPs, furins, cathepsins) are required for fusion activation. Given that these proteases are uniquely present in particular cell types, the S1/S2 cleavages might influence MERS-CoV cell tropism.

Results

S1/S2 Cleavage Is Necessary for MERS-CoV to Infect Calu3 Cells. To evaluate the consequences of S proteolytic cleavage on virus infection, we engineered site-specific S1/S2 mutations ($\underline{R}SV\underline{R}_{751}/S$ in Fig. 1*B*). The WT S1/S2-encoding region was replaced with the codons ($YSAS_{751}/S$) from a MERS-CoV–related bat CoV-HKU4 (Hong Kong University 4). Of note, HKU4 S proteins are secreted from cells as uncleaved forms (31). Additionally, we mutated the R_{748} codon to serine ($S_{748}SV\underline{R}_{751}/S$), expecting that these S proteins would secrete as uncleaved forms but remain susceptible to extracellular serine protease cleavage at S1/S2 sites.

These mutations were incorporated into the MERS-CoV genome and recombinant viruses were generated (32). WT and mutant MERS-CoVs, produced in Vero81 cells, were infected into several different target cells, including Vero81, Huh7, and Calu3. These target cells have differing amounts and types of cellular proteases (23, 25, 30, 33), and therefore each cell type might uniquely process MERS-CoV S proteins, generating differential infection. At 5-h postinfection, total RNAs were extracted from the infected cells and the relative amounts of subgenomic nucleocapsid (N) mRNA were quantified as a measure of infection. In Vero81 and Huh7 cells, infections by WT and mutant MERS-CoVs were comparable, with only a modestly reduced infection of the SSVR mutant into Huh7 cells (Fig. 1*C*). However, in Calu3 cells, the mutants produced ∼4 $\log_{10}$ less viral mRNA than WT (Fig. 1*C*). Consistently, WT and mutant MERS-CoVs produced comparable amounts of progeny viruses in Vero81 and Huh7 cells, whereas in Calu3 cells, mutant virus titers were nearly 3 $\log_{10}$ less virus than those of the WT (Fig. 1*D*). Calu3 are human lung adenocarcinoma cells (34). To assess susceptibility of normal human respiratory cells, viruses were infected into primary cultures of well-differentiated human airway epithelia (HAE). Average progeny virus yields from HAE were $\sim 10^{4.4}$ for WT and mutant SSVR viruses, but were significantly lower at $\sim 10^{3.6}$ for mutant YSAS viruses (Fig. 1*E*). These findings demonstrated that the engineered mutations specifically disabled infection into lung-derived Calu3 cells, with replacement of all basic S1/S2 residues also compromising infection into HAE cultures.

Infected cells were also evaluated for cleaved S proteins by Western blotting (35). Partial WT S1/S2 cleavage was evident in all cell types, but the mutant S proteins were either uncleaved or absent (Fig. 1*F*). Collectively, these findings suggested that viruses must undergo a minimal extent of S1/S2 cleavage in producer Vero81 cells to be infectious to target Calu3 cells.

S1/S2 Cleavage Increases MERS S-Mediated Virus-Cell Entry. To discern the mechanisms by which preliminary S1/S2 cleavage increases MERS-CoV infection, we produced HIV- and vesicular stomatitis virus (VSV)-based MERS pseudoparticles (pps) in 293T cells. Upon S-mediated transduction of target cells, these pps express firefly luciferase (Fluc), with Fluc levels providing quantitative measurements of virus-cell entry.

First, the pps were pelleted, and particle-associated S proteins were evaluated by detecting C-terminal epitopes on Western blots. WT MERS-CoV S proteins were mostly cleaved, whereas both mutant S proteins were uncleaved (Fig. 2*A*). When inoculated at equivalent input multiplicities, the uncleaved mutants were specifically compromised for transduction into lung-derived Calu3 cells (Fig. 2*A*) and HAE cells (Fig. 2*B*). These results were comparable to those obtained with infectious viruses, demonstrating that the MERS pseudoparticle (pp) transductions reflect authentic virus entry, and indicating that the S1/S2 cleavages affect infection at the level of virus-cell entry.

Second, the MERS pps were prepared in serum-free 293T media (SFM) and incubated with trypsin before transduction. Trypsin processed the uncleaved fraction of WT S proteins, as well as the uncleaved SSVR mutant S proteins, into fragments at ∼95 kDa (Fig. 2*C*), consistent with scission at the R_{751}/S cleavage site. In contrast, YSAS S proteins were cleaved at an alternative more N-terminal cleavage site, most likely $\underline{RSTR}_{694}/S$ (30), as inferred from the ∼100-kDa C-terminal fragments (Fig. 2*C*). On transduction into Calu3 cells, this trypsin processing was associated with a >100-fold increase in SSVR pp transduction (Fig. 2*C*). In contrast, the WT and YSAS pp transductions were not affected by trypsin (Fig. 2*C*). The fact that the YSAS pps remained incompetent for transduction even after trypsin proteolysis to an ∼100 kDa form suggested that cleavage at a precisely defined S1/S2 site is a prerequisite for Calu3 infection.

Third, MERS pps were produced in the presence of a proprotein convertase inhibitor (PCI, also known as a dec-RVKR-cmk)

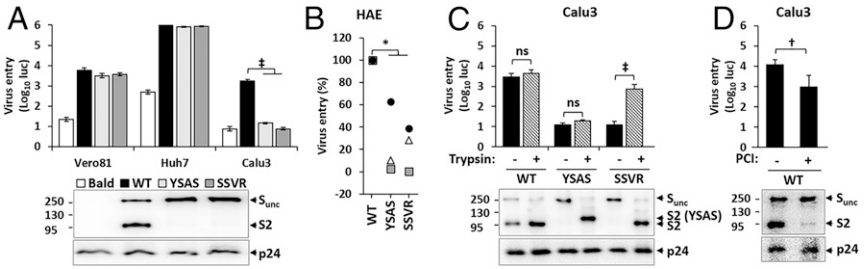

Fig. 2. S1/S2 cleavage is required for MERS pp entry into Calu3 cells. (*A*) Vero81, Huh7, and Calu3 cells were inoculated with WT, S1/S2 mutant (YSAS and SSVR) MERS pps, or with pp-lacking S proteins (Bald). (*B*) Three HAE cultures were inoculated with VSV-based WT and S1/S2 mutant MERS pseudoparticles. (*C*) MERS pps were pretreated with trypsin and then used to inoculate Calu3 cells. (*D*) MERS pps were produced in the presence of PCI, cleared free of residual PCI, and used to inoculate Calu3 cells. In all experiments, virus entry was quantified by measuring luciferase levels at 18 h (*B*) or at 48 h (*A*, *C*, *D*) post-transduction. *Lower* panels depict S proteins on MERS pps after Western blotting. Uncleaved (S_{unc}) and cleaved (S2) positions are indicated. The numbers at the left indicate molecular mass in kilodaltons. Error bars present SD from the mean ($n = 3$). Statistical significance was assessed by Student's *t* test. $^{*}P < 0.05$; $^{\dagger}P < 0.01$; $^{\ddagger}P < 0.001$; ns, not significant.

(36). These pps were concentrated, and pp-associated S proteins were evaluated by Western blotting. Compared with control MERS pps, those secreted from PCI-treated cells contained primarily uncleaved S proteins and were compromised for Calu3 transduction (Fig. 2*D*). These results confirmed that MERS-CoV depends on S1/S2 cleavage by proprotein convertases within 293T producer cells to efficiently infect lung-derived Calu3 target cells.

Preliminary Cleavage Increases SARS S-Mediated Virus-Cell Entry. In contrast to MERS-CoV, which is naturally secreted with cleaved S proteins, the other five human CoV S proteins mediating human lung infections are produced as uncleaved forms (28). Thus, we asked whether preliminary S cleavage facilitates entry by these naturally uncleaved CoVs. HIV-based pps bearing SARS-CoV or human CoV strain 229E S proteins were produced in SFM and treated with trypsin before virus entry. Trypsin processed the SARS S, but not the 229E S proteins, into ~100-kDa fragments, consistent with SARS S cleavage into S1 and S2 (Fig. 3*A*). Without trypsin, the SARS and 229E pps did not transduce Calu3 cells; trypsin exposure before virus inoculation significantly and specifically increased only the SARS pp transduction (Fig. 3*B*). The correlation between S1/S2 proteolysis and Calu3 transduction thus applied to both MERS and SARS pps, suggesting that these two pathogenic human CoVs expand their infection through preliminary S cleavage.

Preliminary Cleavage Facilitates Subsequent S Proteolysis After Receptor Binding. For SARS-CoV and some murine CoVs, the target-cell proteases triggering membrane fusion operate only after the viruses have bound to receptors (2), suggesting that receptor binding induces conformational changes that display S cleavage sites to proteases. We hypothesized that the MERS-CoV S proteins also respond to receptor binding by changing conformation, in ways that are facilitated by prior S1/S2 cleavages. To address this hypothesis, we used an in vitro assay that imitates the structural changes occurring during virus-cell entry. In the assays, MERS pps were incubated on ice with fivefold molar excess of membrane-anchored DPP4 (DPP4 pps), allowing S proteins to bind their cognate receptors. The mixed pps were then digested with trypsin, a surrogate for MERS-CoV activating proteases (33), and S fragmentation patterns were analyzed by Western blotting. In the absence of DPP4, trypsin cleaved the WT S proteins at the S1/S2 cleavage site, and at higher doses, cleaved further to form an ~40-kDa fragment (Fig. 4*A*). However, in the presence of DPP4, trypsin uniquely generated a stable ~72-kDa fragment (Fig. 4*A*), consistent with cleavage at the fusion-activating S2′ site (25). These findings suggested that specific biologically meaningful cleavage sites are exposed in response to receptor binding.

We carried out similar experiments with YSAS MERS pps, expecting that these uncleaved pps would be less susceptible to the receptor- and trypsin-driven S2′ cleavage. Indeed, we observed only barely detectable amounts of YSAS S2′ fragments, even at the high trypsin doses that cleave the majority of receptor-bound WT S proteins into S2′ fragments (Fig. 4*B*). These data indicate that the receptor-promoted exposure of the S2′ cleavage site depends on a prior S1/S2 cleavage.

S1/S2 Cleavage Facilitates Early Virus Entry. On the basis of the in vitro findings in Fig. 4, we hypothesized that S1/S2-cleaved MERS-CoVs would be further processed by target cell proteases shortly after receptor binding, whereas uncleaved MERS-CoVs would traffic onward to endosomes without being sufficiently processed, and would thus be dependent on late endosomal proteases. The proteases cleaving S proteins early after virus binding to target cells include serine-class transmembrane proteins (TMPRs) and furin/proprotein convertases (24, 37, 38), whereas those cleaving S proteins later, after virus endocytosis, include cysteine-class cathepsins (26). Therefore, early and late CoV-cell entry can be distinguished by their sensitivities to serine- and cysteine-specific protease inhibitors, respectively.

We evaluated MERS pp transductions in the presence of camostat, a serine-class TMPR protease inhibitor (23), PCI, an inhibitor of kexin-type proprotein convertases including furin (36), and E64d, an inhibitor of cysteine-class proteases including endosomal cathepsins (39). These inhibitors had no effect on VSV glycoprotein (G)-mediated transductions, but they did reduce MERS S transductions in cell-type–specific fashion (Fig. 5*A* and Fig. S1). In Calu3 cells, camostat, PCI, and E64d blocked transductions ~100-, ~10-, and ~2-fold, respectively, indicating utilization of the early-acting proteases (Fig. 5*A*). Similar patterns were observed during transduction of HAE cultures, with camostat and PCI, but not E64d blocking virus entry (Fig. 5*B*). Conversely, in Huh7 cells camostat was inert, and PCI and E64d effected ~fivefold reductions, a reverse pattern relative to Calu3 cells that suggested utilization of the later-acting proteases (Fig. 5*A*). MERS pp transductions into Caco2 and Vero81 cells were also sensitive to inhibitors of later-acting proteases (Fig. S1).

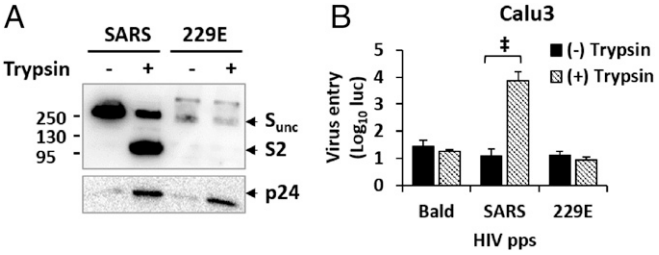

Fig. 3. SARS-CoV S cleavage by trypsin facilitates entry into Calu3 cells. (*A*) SARS and HCoV-229E pps were treated with trypsin. S proteins on pps were analyzed by Western blot. Uncleaved (S_{unc}) and cleaved (S2) positions are indicated. The numbers at the left indicate molecular mass in kilodaltons. (*B*) Calu3 cells were incubated with trypsin pretreated pps. Virus entry was quantified by measuring luciferase levels at 48-h posttransduction. Error bars present SD from the mean ($n = 4$). Statistical significance was assessed by Student's *t* test. $^{\ddagger}P < 0.001$.

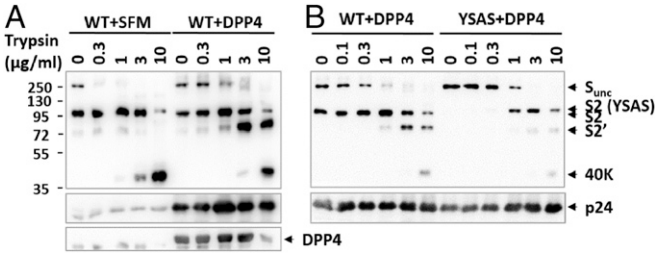

Fig. 4. S1/S2 cleavage facilitates the receptor-induced exposure of a second S2′ cleavage site. (*A*) MERS (WT) pps were mixed with SFM or with DPP4 pps. The mixed pps were treated with increasing concentrations of trypsin. S and DPP4 proteins on pps were analyzed by Western blotting. Uncleaved (S_{unc}) and cleaved (S2, S2′, and 40K) positions are indicated. The numbers at the left indicate molecular mass in kilodaltons. (*B*) Similar experiments to *A* were carried out in parallel with YSAS MERS pps.

In determining whether uncleaved MERS pps were differentially sensitive to these protease inhibitors, we chose to use Huh7 cells, as they supported WT and uncleaved mutant MERS-CoVs nearly equally (Figs. 1 and 2). In these cells, the WT and uncleaved mutant MERS-CoVs were similar in their resistance to camostat, and in their modest sensitivity to PCI, but were set apart by the mutants' hypersensitivity to E64d (Fig. 5*C*). This pattern, in which E64d potently blocked the mutant pp transductions, was also observed in Caco2 cells (Fig. S2). These findings indicated that the uncleaved viruses required a late endosomal cell entry pathway. We considered whether the uncleaved mutant pps might use early-acting proteases if they were provided in abundance. To this end, we overexpressed the TTSP family TMPR serine 2 (TMPRSS2) in Huh7 cells, and then evaluated MERS pp transductions. TMPRSS2 overexpression increased Fluc accumulation (about eightfold) and made all MERS pp transductions slightly sensitive to camostat, and also rendered WT MERS pp transduction completely resistant to E64d (Fig. 5*C*), indicating ample supplies of the TMPRSS2 proteases. However, the overexpressed TMPRSS2 did not render the uncleaved YSAS and SSVR MERS pp transductions resistant to E64d (Fig. 5*C*), indicating that the uncleaved MERS-CoVs are dependent on late-acting cathepsin proteases even when early-acting proteases are abundantly available.

Cathepsin L Sensitizes Calu3 Cells to Uncleaved MERS Viruses. Because uncleaved MERS viruses require late proteases and do not infect Calu3 cells, we inferred that Calu3 cells are depleted in endosomal cathepsins, at least relative to infectable Huh7 cells. This inference was validated by measuring protease-encoding transcripts by quantitative RT-PCR. Huh7 cells contained DPP4, furin, cathepsin L, and cathepsin B, but very few TMPRSS2 transcripts (Fig. 6*A*). Relative to the Huh7 cells, the lung and airway-derived Calu3 and HAE cultures had far more TMPRSS2, but significantly fewer furin and cathepsin L transcripts (Fig. 6*B*). To determine whether the relatively low levels of late-acting proteases in Calu3 cells accounted for virus resistance, we transduced the cells with human cathepsin L genes and then evaluated MERS pp entry. Transduced cells were highly sensitized to uncleaved MERS pp entry, and were made resistant by E64d (Fig. 6*C*). Similar augmentation of uncleaved MERS transduction was achieved by exposing cell-bound MERS pps to purified human cathepsin L (Fig. 6*D*). These results indicate that uncleaved viruses can only infect cells containing sufficient late-acting endosomal proteases, and they make it clear that CoV–cell tropism is related to the abundance and distribution of proteases in both virus-producing and virus-targeting cells.

Discussion

CoV–cell entry can be viewed in the context of a proteolytic cascade that includes at least two cleavages in S proteins, first at S1/S2, then at S2′. For MERS-CoV, the cascade can begin shortly after virus morphogenesis in virus-producing cells. Extensive S1/S2 cleavage at this beginning stage allows for a similarly extensive S2′ cleavage shortly after virus binding to receptors in virus-target cells, and the cascade ends when a sufficient number of adjacent S proteins are triggered for fusion activation by early-acting proteases. However, for several CoVs, and for some variant forms of MERS-CoV, the cascade begins when viruses bind target cells, and then ends much later after virus endocytosis and late-acting intraendosomal proteolysis to activate a sufficient number of adjacent S proteins into fusion competence. These variations in the beginning and ending stages of the CoV infection-related proteolytic cascade are illustrated in Fig. 7.

The beginning and ending points of this proteolytic cascade correlated with cell tropism. MERS-CoVs that began proteolysis at S1/S2 in virus-producing cells could infect Calu3 cells, but mutant MERS-CoVs that remained uncleaved could not (Figs. 1 and 2). Uncleaved MERS viruses bypassed early proteases (Fig. 5*C*) and required late proteases (Fig. 6 *C* and *D*), making it clear that S1/S2 cleavage promotes early entry. Of note, uncleaved viruses were able to infect the more cathepsin protease-enriched Huh7 and Vero81 cells (Figs. 1 and 2). Earlier reports used similar cathepsin-enriched target cell types in their experiments, and thus came to conclusions that the preliminary S1/S2 cleavages had a limited relevance to infection (20, 29, 30). It was the paucity of virus-activating endosomal proteases in Calu3 cells that revealed a key importance for the S1/S2 cleavages in cell tropism.

The relevance of the S1/S2 cleavages extended to infection of primary HAE cultures, as evidenced by the poor growth of the YSAS uncleaved mutant MERS-CoVs (Fig. 1*E*) and the relatively inefficient entry of the YSAS and SSVR uncleaved pseudoviruses (Fig. 2*B*). The WT-level growth of the SSVR mutants might argue against the importance of S1/S2 cleavages in HAE infections; however, we note that HAE are frequently collected from patients with underlying pulmonary diseases (e.g., chronic obstructive pulmonary disease, cystic fibrosis, pulmonary fibrosis, α-1 antitrypsin deficiency), conditions associated with increased levels of mucus-associated proteases (40–42). Airway mucus-associated proteases are known to cleave SARS-CoV S proteins (43), and therefore we suggest that the SSVR mutant MERS-CoVs are similarly cleaved by extracellular proteases, making their infection resemble that of WT viruses at the point of entry into some HAE cells.

Once on Calu3 or HAE target cells, the precleaved viruses are presumably processed to fusion-ready S2′ products by early cell-surface serine proteases (Fig. 5*A*) (23). That uncleaved viruses are not similarly processed by these proteases is best explained by their failure to respond to receptor binding, which limits downstream S2′ processing. MERS S protein interactions with

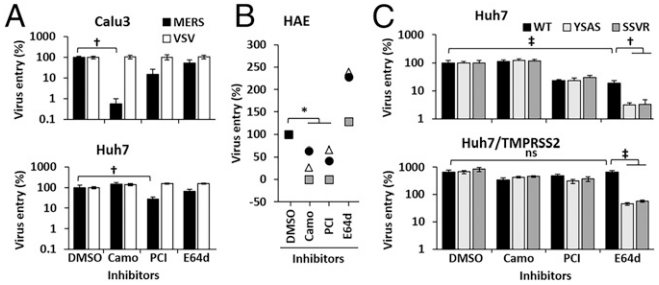

Fig. 5. S1/S2 cleavage facilitates early virus entry. (*A*) Calu3 and Huh7 cells were incubated with protease inhibitors [100 μM camostat (camo), 50 μM PCI, 10 μM E64d], or with DMSO, and then transduced with MERS or VSV pps. (*B*) Three HAE cultures were incubated with indicated protease inhibitors, and then transduced with WT and S1/S2 mutant MERS pps. (*C*) Huh7 and Huh7/TMPRSS2 cells were incubated with protease inhibitors, and then transduced with WT or S1/S2 mutant (YSAS or SSVR) MERS pps. Virus entry was quantified by measuring luciferase levels in infected cells at 48-h (*A*, *C*) or 18-h (*B*) post-transduction. Error bars present SD from the mean ($n = 3$). Statistical significance was assessed by Student's *t* test. $^{*}P < 0.05$; $^{\dagger}P < 0.01$; $^{\ddagger}P < 0.001$; ns, not significant.

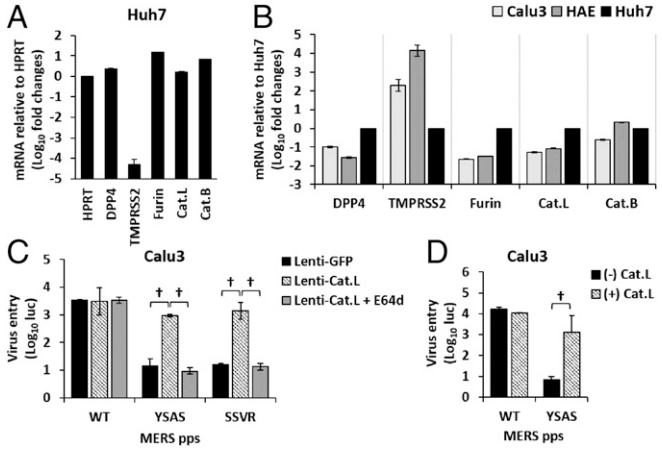

Fig. 6. Uncleaved MERS entry depends on endosomal cathepsins. (*A*) DPP4, TMPRSS2, furin, cathepsin L (Cat. L), cathepsin B (Cat. B), and hypoxanthine phosphoribosyltransferase (HPRT) mRNA levels were measured in Huh7 cell extracts by quantitative RT-PCR, and plotted relative to HPRT. (*B*) The same mRNA levels were measured in Calu3 and HAE cell extracts and plotted relative to those in Huh7 cells. (*C*) Calu3 cells were transduced with lentiviral vectors encoding human cathepsin L or GFP. After 3 d, cells were treated with or without 10 μM E64d and then transduced with WT or S1/S2 mutant MERS pps. (*D*) Calu3 cells were incubated with WT or YSAS MERS pps at 4 °C, and then treated with cathepsin L. Virus entry was quantified by measuring luciferase levels at 48-h posttransduction. Error bars present SD from the mean ($n = 3$). Statistical significance was assessed by Student's t test. $^{\dagger}P < 0.01$.

DPP4 were necessary to reveal a proteolytic cleavage site at or near the S2′ position (Fig. 4*A*), demonstrating that a receptor-induced allosteric transition makes the S2′ cleavage site available to a protease. This DPP4-induced structural transition was far less effective in the absence of the preliminary S1/S2 cleavage (Fig. 4*B*). All of these findings fit well with the model in Fig. 7, which depicts the precleaved viruses transiting rapidly from receptor binding to fusion, whereas uncleaved viruses require more protease and more time to make this transit, and therefore do so only after being trafficked into protease-enriched endosomes.

The recent 4A resolution structures of murine CoV (MHV) and human CoV (HKU-1) S proteins depict uncleaved ectodomain trimers, without ligation to receptors (16, 17). Although images of S proteins in complex with cellular receptors will add important insights, the current structures do suggest that receptor binding locks relatively dynamic S proteins into conformations that expose cleavage sites to host proteases. S1/S2 cleavage may increase the dynamic properties of S proteins, giving them more opportunities to assume locked receptor-bound conformations, making the S2′ sites more rapidly available to proteases. A theme here is that S protein dynamics, achieved through proteolysis or through destabilizing mutations (44), may generally allow for early, cell-surface cleavage at the activating S2′ sites. Of note, such destabilizing mutations are liable to be counter-selected during in vitro virus growth in many cell cultures. In vitro conditions typically select for extracellular virion stability, which maintains infectivity in culture fluids. Therefore, the adaptive mutations fixed into CoV S proteins during in vitro virus propagation may restrict dynamic structural transitions (45). These in vitro mutations are frequently attenuating in in vivo CoV infection models (46). We suggest that in vivo attenuation arises because the stabilized viruses have reduced capacities to assume the receptor-bound conformations enabling S2′ proteolysis and fusion activation. The stabilized, cell culture-adapted CoVs are therefore directed to the late endosomal entry routes, which may correlate with diminished capacities to infect many of the target cells found in in vivo environments.

Several CoVs, including SARS- and human 229E-CoVs, remain uncleaved throughout their morphogenesis and secretion from virus-producing cells (27, 28). Thus, several CoV S proteins remain in their more rigidly structured uncleaved forms until target cell entry. For these less flexible viruses to transit into protease-sensitive and fusion-competent forms, they may need the energy derived from high-affinity interactions with receptors. Indeed the affinity of SARS-CoV S with its receptor angiotensin converting enzyme 2 (ACE2) is 10- to 20-fold higher than that of MERS-CoV S with its receptor DPP4 (47, 48). Thus, one can suggest that S1/S2-cleavages may reduce the need for high-specificity receptor interactions, and in doing so, may allow CoVs to bind adaptably to receptor orthologs, fostering zoonoses. Consistent with this hypothesis, the human-circulating MERS-CoVs have not undergone significant adaptations in their RBDs, at least not toward higher-affinity binding to DPP4. In fact, one lineage of human MERS-CoVs acquired reduced affinity to DPP4 (49). This finding contrasts with the SARS-CoV epidemics of 2003–2004, where adaptive changes increased binding affinities to ACE2 (50). Receptor utilization in relation to S proteolytic processing will inform us on CoV transmissions.

Recent excellent reports have made connections between CoV S proteolytic processing and CoV virulence. For example, CoV S protein proteolytic processing, principally by TMPRSS2, was suggested to increase viral pathogenesis by generating S "decoy" fragments that bind and sterically inactivate antiviral antibodies (24). Additionally, S protein proteolysis, again by TMPRSS2, was suggested to increase pathogenesis by allowing viruses to bypass IFN-induced transmembrane protein 3, an innate antiviral effector that blocks virus-endosome membrane fusions (51, 52). Here we claim that MERS-CoVs, and other CoVs, will preferentially use TMPRSS2 if they have been precleaved; that is, preliminary S1/S2 proteolysis gives infecting viruses the facility to use TMPRSS2 and other early-acting proteases for fusion activation. Thus, the preliminary S1/S2 cleavages may be the more proximal determinants of pathogenesis. Of the six known human CoVs, only MERS-CoV secretes from virus-producing cells with cleaved S proteins, and SARS-CoV, secreted uncleaved, can be processed by extracellular proteases before encountering target cells (Fig. 3) (1). Therefore, these viruses have special facility for using early-acting entry proteases. Preliminary S cleavages may also contribute to the tissue tropism and pathogenesis of feline and murine CoVs (4). As human CoVs continue to infect humans, it will be important to consider possible adaptive changes in their S protein proteolytic processing cascades, as these may contribute to CoV disease.

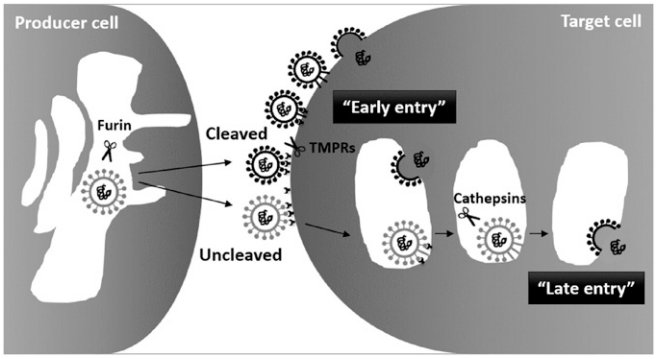

Fig. 7. MERS-CoV–cell entry model. In some producer cell types, MERS-CoV S proteins are cleaved by furin/proprotein convertases in the exocytic pathway. Cleaved MERS-CoV S proteins change their conformations rapidly after receptor binding, exposing subsequent proteolytic cleavage sites, which are processed by proteases (i.e., TMPRs, found at or near cell surfaces). Early cell-surface entry is achieved when several adjacent S proteins are processed. In other producer cell types, MERS-CoV S proteins are not cleaved. Uncleaved MERS-CoV S proteins slowly change their conformations after receptor binding. MERS-CoVs having uncleaved S proteins traffic to the late endosomes/lysosomes and late endosomal entry is achieved when several adjacent S proteins are eventually processed by cathepsins.

Experimental Procedures

Recombinant MERS-CoV Production and Infection. Recombinant WT and mutant MERS-CoVs were generated from bacterial artificial chromosomes and infected into Vero81, Huh7, and Calu3 cells or HAE cultures. HAE cultures were obtained from the University of Iowa Cell Culture Core Facility, which acquired tissue by informed consent under an Institutional Review Board-approved organ research donation protocol. Virus infectivities were analyzed by real-time RT-PCR and by plaque assay.

HIV and VSV Pseudoparticle Transduction. Viral psueudoparticles were transduced into Vero81, Huh7, Calu3, or HAE cultures, with or without prior protease or protease inhibitor exposures. Fluc levels were measured posttransduction.

In Vitro S Fragmentation Assay. MERS pps and DPP4 pps were incubated in 1:5 M ratios, digested with graded doses of trypsin, and S fragments visualized by Western blotting.

For additional information, see *SI Experimental Procedures*. See Tables S1–S3 for primers used for MERS-CoV, real-time PCR, and mutant MERS pps.

ACKNOWLEDGMENTS. We thank Edward Campbell for lentiviral vectors; Michael Hantak, James Earnest, and Enya Qing for helpful discussions; and the University of Iowa In Vitro Models and Cell Culture Core for primary human airway epithelia cultures. This work was supported by NIH Grant P01 AI 060699. The University of Iowa Cell Culture Core is supported by NIH Grants P01 HL51670, P01 HL091842, P30 DK54759, and by the Cystic Fibrosis Foundation. P.B.M. is supported by the Roy J. Carver Charitable Trust.

1. Belouzard S, Chu VC, Whittaker GR (2009) Activation of the SARS coronavirus spike protein via sequential proteolytic cleavage at two distinct sites. *Proc Natl Acad Sci USA* 106(14):5871–5876.
2. Matsuyama S, Taguchi F (2009) Two-step conformational changes in a coronavirus envelope glycoprotein mediated by receptor binding and proteolysis. *J Virol* 83(21):11133–11141.
3. Chandran K, Sullivan NJ, Felbor U, Whelan SP, Cunningham JM (2005) Endosomal proteolysis of the Ebola virus glycoprotein is necessary for infection. *Science* 308(5728): 1643–1645.
4. Licitra BN, et al. (2013) Mutation in spike protein cleavage site and pathogenesis of feline coronavirus. *Emerg Infect Dis* 19(7):1066–1073.
5. Kido H, et al. (2012) Role of host cellular proteases in the pathogenesis of influenza and influenza-induced multiple organ failure. *Biochim Biophys Acta* 1824(1):186–194.
6. Zhou Y, et al. (2015) Protease inhibitors targeting coronavirus and filovirus entry. *Antiviral Res* 116:76–84.
7. Weiss SR, Navas-Martin S (2005) Coronavirus pathogenesis and the emerging pathogen severe acute respiratory syndrome coronavirus. *Microbiol Mol Biol Rev* 69(4):635–664.
8. Annan A, et al. (2013) Human betacoronavirus 2c EMC/2012-related viruses in bats, Ghana and Europe. *Emerg Infect Dis* 19(3):456–459.
9. Lau SK, et al. (2005) Severe acute respiratory syndrome coronavirus-like virus in Chinese horseshoe bats. *Proc Natl Acad Sci USA* 102(39):14040–14045.
10. Li W, et al. (2005) Bats are natural reservoirs of SARS-like coronaviruses. *Science* 310(5748):676–679.
11. Guan Y, et al. (2003) Isolation and characterization of viruses related to the SARS coronavirus from animals in southern China. *Science* 302(5643):276–278.
12. Webster RG (2004) Wet markets—A continuing source of severe acute respiratory syndrome and influenza? *Lancet* 363(9404):234–236.
13. Khalafalla AI, et al. (2015) MERS-CoV in upper respiratory tract and lungs of dromedary camels, Saudi Arabia, 2013-2014. *Emerg Infect Dis* 21(7):1153–1158.
14. Assiri A, et al. (2013) Epidemiological, demographic, and clinical characteristics of 47 cases of Middle East respiratory syndrome coronavirus disease from Saudi Arabia: A descriptive study. *Lancet Infect Dis* 13(9):752–761.
15. Peiris JS, Guan Y, Yuen KY (2004) Severe acute respiratory syndrome. *Nat Med* 10(12, Suppl):S88–S97.
16. Kirchdoerfer RN, et al. (2016) Pre-fusion structure of a human coronavirus spike protein. *Nature* 531(7592):118–121.
17. Walls AC, et al. (2016) Cryo-electron microscopy structure of a coronavirus spike glycoprotein trimer. *Nature* 531(7592):114–117.
18. Raj VS, et al. (2013) Dipeptidyl peptidase 4 is a functional receptor for the emerging human coronavirus-EMC. *Nature* 495(7440):251–254.
19. Millet JK, Whittaker GR (2015) Host cell proteases: Critical determinants of coronavirus tropism and pathogenesis. *Virus Res* 202:120–134.
20. de Haan CA, Stadler K, Godeke GJ, Bosch BJ, Rottier PJ (2004) Cleavage inhibition of the murine coronavirus spike protein by a furin-like enzyme affects cell-cell but not virus-cell fusion. *J Virol* 78(11):6048–6054.
21. Yamada Y, Liu DX (2009) Proteolytic activation of the spike protein at a novel RRRR/S motif is implicated in furin-dependent entry, syncytium formation, and infectivity of coronavirus infectious bronchitis virus in cultured cells. *J Virol* 83(17):8744–8758.
22. Wicht O, et al. (2014) Identification and characterization of a proteolytically primed form of the murine coronavirus spike proteins after fusion with the target cell. *J Virol* 88(9):4943–4952.
23. Shirato K, Kawase M, Matsuyama S (2013) Middle East respiratory syndrome coronavirus infection mediated by the transmembrane serine protease TMPRSS2. *J Virol* 87(23):12552–12561.
24. Glowacka I, et al. (2011) Evidence that TMPRSS2 activates the severe acute respiratory syndrome coronavirus spike protein for membrane fusion and reduces viral control by the humoral immune response. *J Virol* 85(9):4122–4134.
25. Millet JK, Whittaker GR (2014) Host cell entry of Middle East respiratory syndrome coronavirus after two-step, furin-mediated activation of the spike protein. *Proc Natl Acad Sci USA* 111(42):15214–15219.
26. Simmons G, et al. (2005) Inhibitors of cathepsin L prevent severe acute respiratory syndrome coronavirus entry. *Proc Natl Acad Sci USA* 102(33):11876–11881.
27. Song HC, et al. (2004) Synthesis and characterization of a native, oligomeric form of recombinant severe acute respiratory syndrome coronavirus spike glycoprotein. *J Virol* 78(19):10328–10335.
28. Zhou W, Wang W, Wang H, Lu R, Tan W (2013) First infection by all four non-severe acute respiratory syndrome human coronaviruses takes place during childhood. *BMC Infect Dis* 13:433–440.
29. Follis KE, York J, Nunberg JH (2006) Furin cleavage of the SARS coronavirus spike glycoprotein enhances cell-cell fusion but does not affect virion entry. *Virology* 350(2):358–369.
30. Gierer S, et al. (2015) Inhibition of proprotein convertases abrogates processing of the Middle Eastern respiratory syndrome coronavirus spike protein in infected cells but does not reduce viral infectivity. *J Infect Dis* 211(6):889–897.
31. Yang Y, et al. (2014) Receptor usage and cell entry of bat coronavirus HKU4 provide insight into bat-to-human transmission of MERS coronavirus. *Proc Natl Acad Sci USA* 111(34):12516–12521.
32. Almazán F, et al. (2013) Engineering a replication-competent, propagation-defective Middle East respiratory syndrome coronavirus as a vaccine candidate. *MBio* 4(5): e00650-13.
33. Qian Z, Dominguez SR, Holmes KV (2013) Role of the spike glycoprotein of human Middle East respiratory syndrome coronavirus (MERS-CoV) in virus entry and syncytia formation. *PLoS One* 8(10):e76469.
34. Fogh J, Fogh JM, Orfeo T (1977) One hundred and twenty-seven cultured human tumor cell lines producing tumors in nude mice. *J Natl Cancer Inst* 59(1):221–226.
35. Zhao J, et al. (2014) Rapid generation of a mouse model for Middle East respiratory syndrome. *Proc Natl Acad Sci USA* 111(13):4970–4975.
36. Fugère M, Day R (2005) Cutting back on pro-protein convertases: The latest approaches to pharmacological inhibition. *Trends Pharmacol Sci* 26(6):294–301.
37. Matsuyama S, et al. (2010) Efficient activation of the severe acute respiratory syndrome coronavirus spike protein by the transmembrane protease TMPRSS2. *J Virol* 84(24):12658–12664.
38. Shulla A, et al. (2011) A transmembrane serine protease is linked to the severe acute respiratory syndrome coronavirus receptor and activates virus entry. *J Virol* 85(2):873–882.
39. Tamai M, et al. (1987) Efficient synthetic method for ethyl (+)-(2S,3S)-3-[(S)-3-methyl-1-(3-methylbutylcarbamoyl)butylcarbamoyl]-2-oxiranecarb oxylate (EST), a new inhibitor of cysteine proteinases. *Chem Pharm Bull (Tokyo)* 35(3):1098–1104.
40. Almansa R, et al. (2012) Critical COPD respiratory illness is linked to increased transcriptomic activity of neutrophil proteases genes. *BMC Res Notes* 5:401–408.
41. Kristensen JH, et al. (2015) Levels of circulating MMP-7 degraded elastin are elevated in pulmonary disorders. *Clin Biochem* 48(16-17):1083–1088.
42. Twigg MS, et al. (2015) The role of serine proteases and antiproteases in the cystic fibrosis lung. *Mediators Inflamm* 2015:293053.
43. Belouzard S, Madu I, Whittaker GR (2010) Elastase-mediated activation of the severe acute respiratory syndrome coronavirus spike protein at discrete sites within the S2 domain. *J Biol Chem* 285(30):22758–22763.
44. Saeki K, Ohtsuka N, Taguchi F (1997) Identification of spike protein residues of murine coronavirus responsible for receptor-binding activity by use of soluble receptor-resistant mutants. *J Virol* 71(12):9024–9031.
45. Scobey T, et al. (2013) Reverse genetics with a full-length infectious cDNA of the Middle East respiratory syndrome coronavirus. *Proc Natl Acad Sci USA* 110(40):16157–16162.
46. Ontiveros E, Kim TS, Gallagher TM, Perlman S (2003) Enhanced virulence mediated by the murine coronavirus, mouse hepatitis virus strain JHM, is associated with a glycine at residue 310 of the spike glycoprotein. *J Virol* 77(19):10260–10269.
47. Wu K, et al. (2011) A virus-binding hot spot on human angiotensin-converting enzyme 2 is critical for binding of two different coronaviruses. *J Virol* 85(11):5331–5337.
48. Lu G, et al. (2013) Molecular basis of binding between novel human coronavirus MERS-CoV and its receptor CD26. *Nature* 500(7461):227–231.
49. Kim Y, et al. (2016) Spread of mutant Middle East respiratory syndrome coronavirus with reduced affinity to human CD26 during the South Korean outbreak. *MBio* 7(2):e00019.
50. Li W, et al. (2005) Receptor and viral determinants of SARS-coronavirus adaptation to human ACE2. *EMBO J* 24(8):1634–1643.
51. Bertram S, et al. (2013) TMPRSS2 activates the human coronavirus 229E for cathepsin-independent host cell entry and is expressed in viral target cells in the respiratory epithelium. *J Virol* 87(11):6150–6160.
52. Huang IC, et al. (2011) Distinct patterns of IFITM-mediated restriction of filoviruses, SARS coronavirus, and influenza A virus. *PLoS Pathog* 7(1):e1001258.
53. Karp PH, et al. (2002) An in vitro model of differentiated human airway epithelia. Methods for establishing primary cultures. *Methods Mol Biol* 188:115–137.